

## Relevance of surrogate-data testing in electroencephalogram analysis

N. Pradhan\* and P. K. Sadasivan

*Department of Psychopharmacology, National Institute of Mental Health and Neurosciences (NIMHANS),  
Bangalore 560 029, India*

(Received 7 August 1995)

Surrogate-data testing has been propounded to detect nonlinearity and chaos in experimental time series and to differentiate them from linear stochastic processes or colored noises. The surrogate tests of brain signals [electroencephalograms (EEG's)] have produced equivocal results. Therefore, we examine the surrogate testing procedure using numerical data of classical chaotic systems, mixed sine waves, white Gaussian and colored Gaussian noises, and EEG's. The white Gaussian noise and chaotic time series are easily discerned by the surrogate-data test. However, the surrogate-data test fails to detect colored Gaussian noise data of low correlation dimensions ( $D_2$ ) or mixed sine waves containing a smaller number of wave forms. The colored Gaussian noise appears linear and stochastic only when there is an increased randomness in its pattern and the data set is high dimensional. Therefore, the "surrogate test" may not be a sufficient test for chaoticity and wrong conclusions can be arrived at if analyses are based only on the surrogate test. The EEG time series produce finite correlation dimensions. The surrogate testing of eight independent realizations of different forms of EEG activities produces significantly different  $D_2$  values (Student's  $t$  test) than the original data sets. Thus the EEG is proven to be chaotic in nature. Apparently many natural phenomena follow deterministic chaos, and as the dimensional complexity of the system increases ( $D_2 > 5$ ) it may be approximated to be stochastic.

PACS number(s): 87.10.+e

### I. INTRODUCTION

Biological systems are poorly defined and investigators face the dilemma of interpreting a system's behavior from the observed experimental time series. Consequent to the recent developments in nonlinear dynamics and the theory of chaos, many biological systems have been found to exhibit chaotic behavior [1-5]. Esthetically a dynamical model driven approach is preferred to a phenomenological stochastic description. Therefore the formalism of chaotic dynamics has found application in understanding brain functions. Brain signals can be recorded by placing electrodes on the scalp surface and these signals reflect the dynamical behavior of the underlying neural structures. The frequency content of an electroencephalogram (EEG) is of importance in its assessment and hence extensive studies have been made based on the frequency analysis of EEG's. Thus we find frequent mention in the EEG literature of four rhythmic activities characterized by their frequency bands, which are designated as  $\delta$  (0.5 to 3 Hz),  $\theta$  (4 to 7 Hz),  $\alpha$  (8 to 13 Hz), and  $\beta$  (14 to 30 Hz) activities. The  $\alpha$  and  $\beta$  EEG activities are normal rhythms. The  $\delta$  and  $\theta$  EEG activities are associated with sleep, altered states of consciousness, or pathological

conditions. The random-looking EEG signals have been examined in the past by spectral estimates or parametric linear modeling with little consideration of the processes that generate these signals [6,7]. EEG signals show dramatic changes in their structure pattern in deep sleep, epilepsy, coma, etc. A linear stochastic model of EEG generation may not account for such transitions, whereas the time evolution of chaotic systems shows transitions from periodic states to aperiodic states. Therefore the concept of chaos introduces a dynamical perspective for understanding brain functions. It has led to the application of nonlinear dynamical measures to the analysis of EEG signals recently. Reference to such applications may be encountered in books on chaos, reviews, and monographs [8-13].

The calculation of the attractor dimension or correlation dimension ( $D_2$ ) of EEG time series has dominated recent literature [9,14-17]. The dimension of the attractor is a characteristic feature of the underlying neuronal processes generating the EEG signals. The  $D_2$  value of the attractor may be of significance in detecting features of various brain states, classification of patterns of neural activities, and identification of specific drug effects on the brain. The attractor dimension directly reflects the degrees of freedom of the system under study. Therefore nonlinear dynamics provides a model for signal generation and temporal prediction which may help in determining the nature of neuronal processes governing brain activity. Results on attractor dimension analysis of EEG's are available in the literature in the normal resting state, epileptic seizures, different sleep stages, and states of anesthesia. Correlation dimension analysis is also available from cases concerning attentional tasks

---

\*Mailing address: Department of Psychopharmacology, National Institute of Mental Health and Neurosciences (NIMHANS), Hosur Road, Bangalore-560 029, India. FAX: 0091-080-6631830.

in humans and experimental learning situations in rats [8–10,18-20]. The human data on the attractor dimension in the resting state have been rather less consistent with a range from 3 to over 10. The dimensionality has been consistently seen to drop during an epileptic epoch and stage IV deep sleep. Difficulties in comparing disparate results arise because of the algorithms used and the definition of dimensionality employed. Certain uniform conventions may emerge for handling experimental time series in future. However, using the parameter of the attractor dimension, a specific predictive model can be built and experimental verification of the model is possible [21]. This newly gained insight into the chaotic dynamics of the brain is a significant departure from the earlier stochastic visualization. Thus nonlinear dynamics may be the method of study for complex systems and their experimental time series. The application of nonlinear methods to EEG analysis has been discussed in detail in a previous paper [22].

The chaos conjecture of EEG's is based on a finite correlation dimension and a positive dominant Lyapunov exponent ( $\lambda_1$ ) of the time series [23,24]. A number of technical problems may cause EEG's to be contaminated with signals from noncerebral sources making the  $D_2$  or  $\lambda_1$  estimation spurious. Therefore the chaos theory of EEG's has been seriously questioned and surrogate-data testing has recently been proposed as one way to detect the presence of nonlinearity and low-dimensional chaos in experimental time series [25–27]. The suggestion for “surrogate-data testing” stems from the observation that linear-stochastic systems (“colored noises”) also result in finite  $D_2$  estimates [28,29] and the surrogate testing may differentiate chaos from colored noises. The details of surrogate testing with numerical test data has been described by Theiler *et al.* [25]. In their observations, one set of EEG's did not show nonlinear structure while another set did show nonlinear structure. Following a similar line of thinking, a number of investigators claim that EEG activity is a colored noise and not chaotic [25,27,30–32].

In this paper, we evaluate the validity of the surrogate-data test using numerical data of the classical chaotic

systems of the Lorenz map and the Hénon map, white Gaussian noises, colored Gaussian noises, and mixture of sine waves along with experimental EEG data.

## II. NUMERICAL AND EXPERIMENTAL DATA SETS

### A. Lorenz map and Hénon map

The well known Hénon map and Lorenz map are the classical examples of chaotic systems. The Lorenz system is given by

$$\begin{aligned}\dot{x} &= cy - cx, \\ \dot{y} &= rx - y - xz, \\ \dot{z} &= bz + xy,\end{aligned}\quad (1)$$

where  $c = 10$ ,  $b = 8/3$ , and  $r = 28$ . Gill's routine is used for integration with a step size of 0.006. The initial conditions  $x(0) = y(0) = z(0) = 1$  are used for the Lorenz map. 200 000 data points are generated, of which 5000 points are discarded to remove the initial transients.

The Hénon map is given by the equation

$$x_{i+1} = bx_{i-1} + 1 - ax_i^2, \quad (2)$$

where  $a = 1.4$  and  $b = 0.3$ . 90 000 data samples are generated using the initial conditions  $x_i = x_{i-1} = 0.0$  for the Hénon map. The initial 5000 data points are discarded to avoid transients at the beginning of the data. The Lorenz map ( $x$  component) and the Hénon map data, the corresponding surrogate-data sets, and the power spectra are shown in Fig. 1

### B. Mixed sine waves

The standard sine function is used to generate varying points of sine waves.

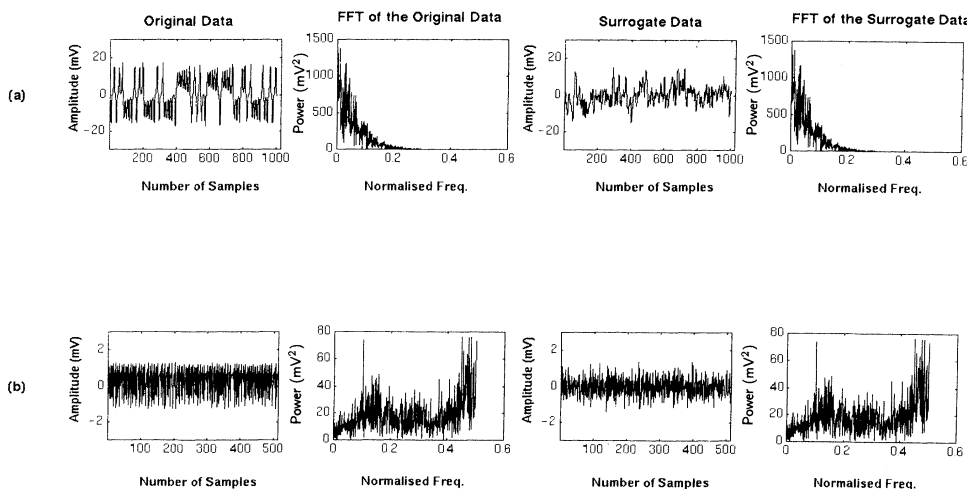


FIG. 1. The numerical data of chaotic systems. (a) Lorenz map ( $x$  component) and (b) Hénon map; the original data and the surrogate-data sets with the corresponding power spectra.

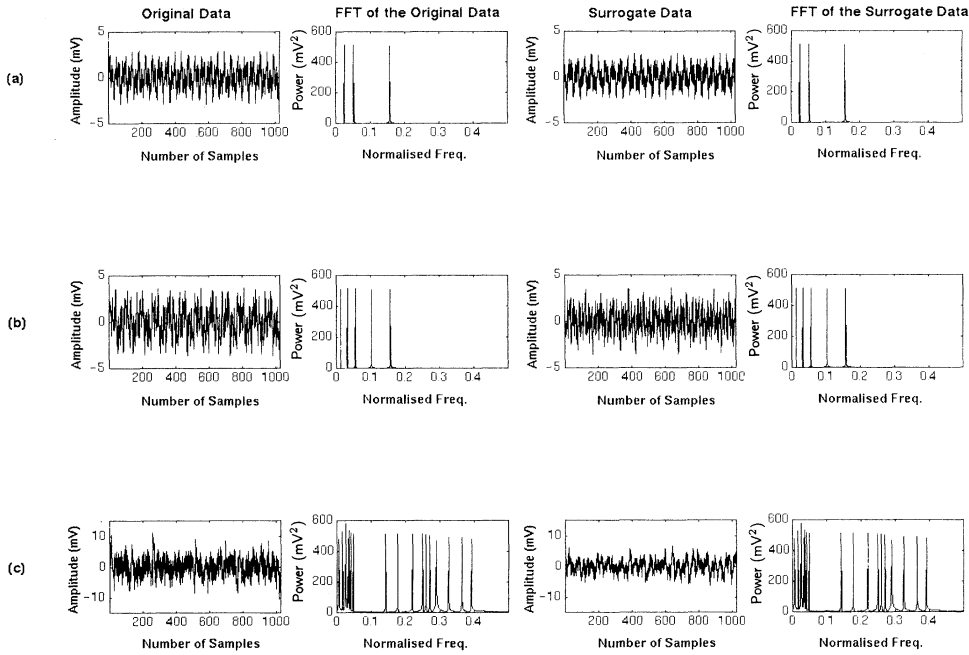


FIG. 2. The numerical data of mixed sine waves. A mixture of (a) three (b) five, and (c) 20 sinusoidal wave forms; the original data and surrogate-data sets with the corresponding power spectra.

$$X_i = \sin \left[ \frac{2\pi f_i}{f_s} \right], \quad (3)$$

where  $f_i$  denotes the frequency (randomly chosen in the range 0.5–100 Hz) of the  $i$ th sinusoid and  $f_s$  the number of data samples per cycle. Eight realizations of each

mixed sinusoid (mixture of 3, 5, and 20 wave forms) are generated. The resulting signals are made to have zero mean and unit variance. The probability distribution is almost Gaussian. The signals, the corresponding surrogate-data sets, and the power spectra are given in Fig. 2.

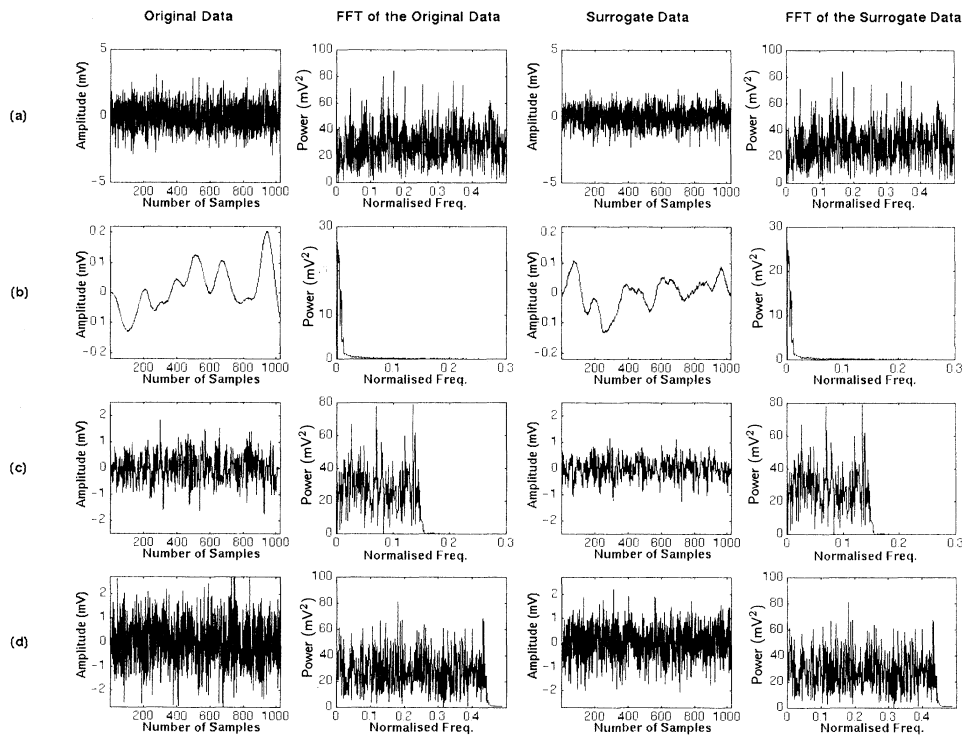


FIG. 3. The numerical data of (a) white Gaussian noise, (b) colored Gaussian noise generated by low-pass filtering the white Gaussian noise at 3 Hz cutoff frequency, (c) colored Gaussian noise generated by low-pass filtering the white Gaussian noise at 300 Hz cutoff frequency, and (d) colored Gaussian noise generated by low-pass filtering the white Gaussian noise at 900 Hz cutoff frequency; the original data and surrogate-data sets with the corresponding power spectra.

### C. White Gaussian noises and colored Gaussian noises

Normally distributed random numbers of zero mean and unit variance are generated as white Gaussian noise. The signal, its surrogate-data sets, and the spectrum are given in Fig. 3(a). Colored Gaussian noises are generated by applying linear phase low-pass finite impulse response (FIR) filters and varying cutoff frequencies from 3 Hz to 900 Hz. The representative 3, 300, and 900 Hz colored noises, the corresponding surrogate-data sets, and the power spectra are shown in Figs. 3(b), 3(c), and 3(d), respectively.

### D. Experimental data

EEG data were collected from the eight loci of the international 10-20 system using a conventional EEG machine coupled to a 486 PC-AT system with analog to digital converters (DT2841) and array processors (DT7020) of Data Translation Inc. Seven normal male subjects having no history of neurologic or psychiatric disorders participated [mean age 28.5 yr, (SD) 3.25, range 22–35]. Subjects were tested in the morning in a soundproof, electrically shielded room while lying on a comfortable bed. Silver cup electrodes were attached to the eight scalp loci ( $Fp_1$ ,  $F_7$ ,  $T_3$ ,  $O_1$  with reference electrode at  $A_1$ ,  $Fp_2$ ,  $F_8$ ,  $T_4$ ,  $O_2$  with reference electrode  $A_2$ , and the forehead the ground electrode) for monopolar recording. They were

instructed to be in a relaxed state with eyes open for 15 min and then eyes closed for 15 min. On-line digital recording was continued for 30 min for each subject and the procedure was repeated four times on the same subject. The same subjects were also taken for a whole night sleep recording [one channel of EEG  $C_3-A_1$ , one channel of electromyogram (EMG), two channels of electrooculogram (EOG)], after two nights of acclimatization. The procedure described by Rechtschaffen and Kales [33] was followed. The whole night digital data of the seven subjects were obtained.

The EEG signals were digitized at 128 samples/sec to the PC-AT and later ported to a HP-9000/735 graphics workstation. The signals were filtered through a band-pass filter (0.5–32 Hz by fourth order Butterworth twice cascaded) prior to analysis. The data of each subject were visually screened to obtain artifact free data of at least 8 sec duration in various traditional EEG activity bands. The data blocks were classified as  $\alpha$ ,  $\beta$ , and indeterminate activity patterns with the help of two experienced electroencephalographers who differed by < 5% in their scoring. The differences were resolved by discussion and consensus rating. The sleep EEG data were screened to obtain  $\theta$  and  $\delta$ , sleep activity patterns. A representative sample of  $\alpha$ ,  $\beta$ ,  $\theta$ ,  $\delta$  and indeterminate EEG activities, the corresponding surrogate-data sets, and the power spectra is given in Fig. 4. Eight independent realizations of different activity patterns of EEG's are used for estimation of the correlation dimension and surrogate testing.

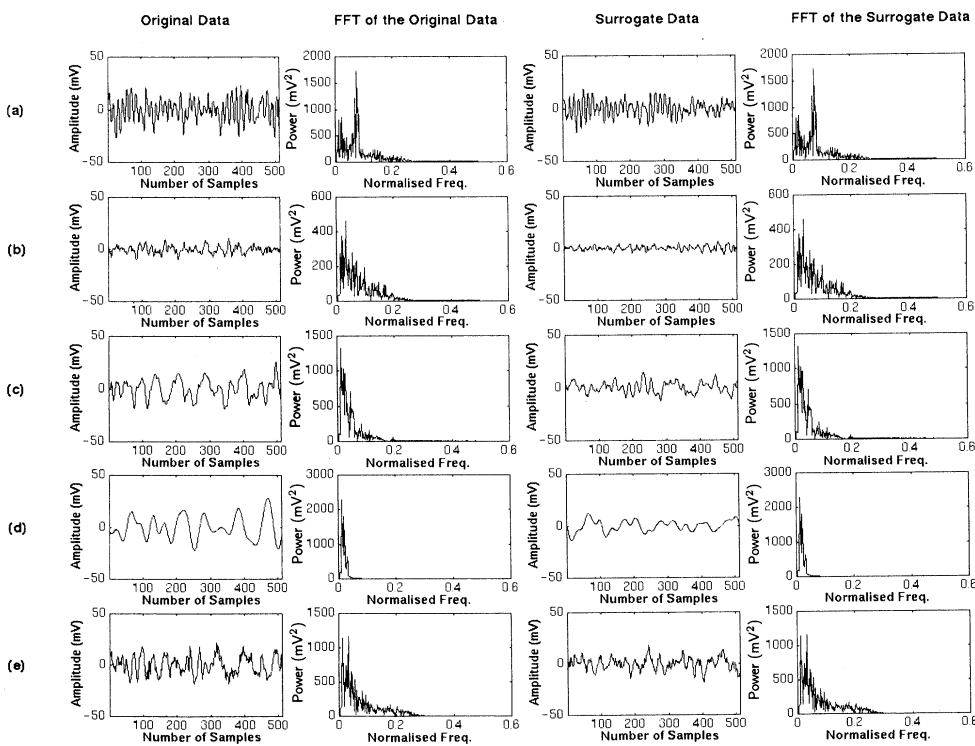


FIG. 4. The experimental EEG data of (a)  $\alpha$  activity, (b)  $\beta$  activity, (c)  $\theta$  activity, (d)  $\delta$  activity; and (e) indeterminate activity; the original data and surrogate-data sets with the corresponding power spectra.

### III. ESTIMATION OF $D_2$ AND SURROGATE-DATA TESTING

We have employed the maximum-likelihood  $D_2$ -estimation method developed by Takens [34] and extended by Ellner [35]. The Takens-Ellner algorithm is chosen over the Grassberger-Procaccia algorithm for its computational efficiency and its use for small data sets [27].  $D_2$  is estimated for embedding dimensions 4–16 for all data. The same data sets are subjected to the surrogate test as employed by Theiler *et al.* [25] in their investigations of real and simulated data (no windowing, original amplitudes, type-II surrogating). The surrogate data are designed to test the null hypothesis that, although the dynamics of the observed signal is linear, it may be subject to nonlinear distortions. The original signal  $x_t$  is transformed into  $y_t$  by a static nonlinear filter  $H(\cdot)$ . The filter is static in the sense that  $y_t$  depends only on the current value of  $x_t$ . First a time series  $g_t$  having an independent identical Gaussian distribution is formed. Next, we reorder  $g_t$  so that its ranking agrees with the transformed time series  $y_t$ ; that is, if  $y_{t=i}$  is the  $n$ th smallest of all the  $y$ 's, then  $g_{t=i}$  will be the  $n$ th smallest of all the  $g$ 's. Therefore the reordered  $g_t$  is a time series which follows the time series  $y_t$  and has a Gaussian amplitude

distribution. The  $g_t$  is then Fourier transformed, phase-angle shuffled, and inverse Fourier transformed to form  $g'_t$ , a surrogate of the Gaussian time series. The final surrogate is obtained by reordering  $y_t$  so that it follows  $g'_t$  [25,32].

Sixteen such phase shuffled surrogate sets are generated for a single set of original data. A minimum of eight original data sets are evaluated for surrogate testing in each category. The surrogate  $D_2$  values are statistically compared (Student's  $t$  test) with the  $D_2$  values of the original signals across the embedding dimensions.

## IV. RESULTS

### A. Chaotic time series

The Lorenz map and Hénon map clearly show saturation of their  $D_2$  values for embedding dimension 6–16. The  $D_2$  curves of the original data of Lorenz ( $x$  component) for different embedding dimensions and the surrogate-data sets are given in Fig. 5(a). The  $D_2$  curve of the original data levels off at embedding dimension 6. The corresponding surrogate-data sets do not show significant saturation in  $D_2$  values with increasing embed-

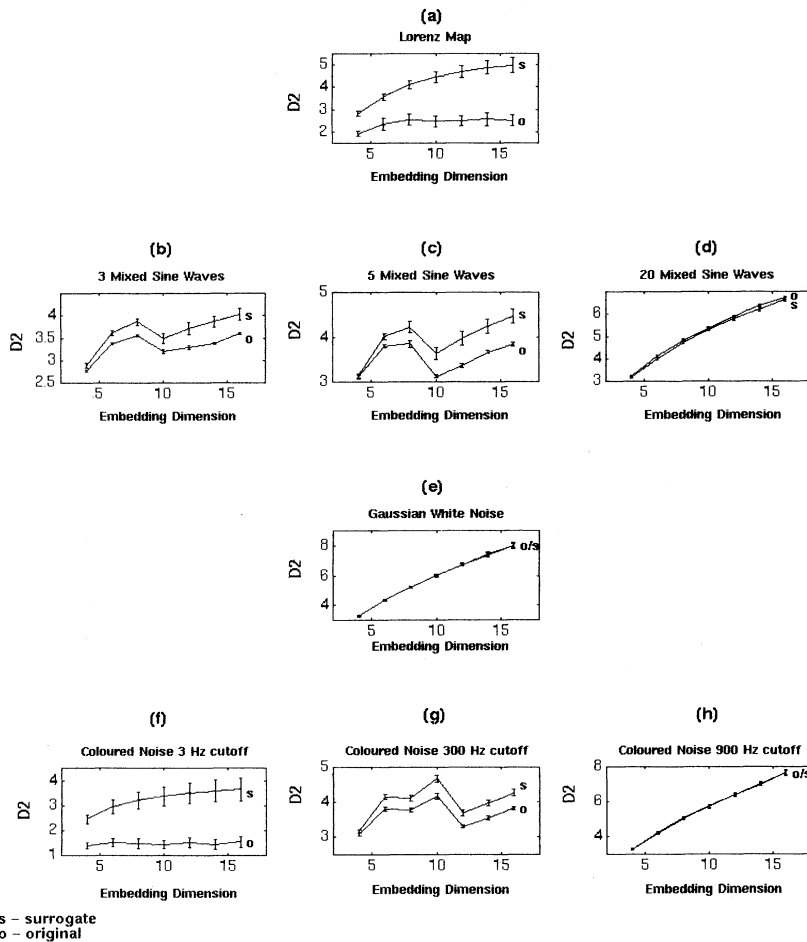


FIG. 5. The estimated  $D_2$  for original data sets (o) and the corresponding surrogate-data sets (s) for the numerically generated data of (a) Lorenz map, (b) three mixed sine waves, (c) five mixed sine waves, (d) 20 mixed sine waves, (e) white Gaussian noise, (f) colored Gaussian noise at 3 Hz cutoff, (g) colored Gaussian noise at 300 Hz cutoff, and (h) colored Gaussian noise at 900 Hz cutoff.

ding dimensions. The  $D_2$  values of the surrogate data are significantly higher than the original sets ( $p < 0.01$ ) for all embedding dimensions for both Lorenz and Hénon data.

### B. Mixed sine waves

The mixed sine waves constituting 20 different sinusoidal wave forms do not have a saturable or finite correlation dimension [Fig. 5(d)]. The surrogate-data sets show similar behavior in  $D_2$  values. However, the  $D_2$  values of the surrogate sets are significantly different from the original data sets ( $p < 0.001$  for embedding dimensions 4, 6, 8, and 14,  $p=0.03$  at embedding dimension 10,  $p=0.0025$  at embedding dimension 12, and  $p=0.0097$  at embedding dimension 16). The mixed sine waves with fewer sinusoids (three and five) display saturation of  $D_2$  values [Figs. 5(b) and 5(c)] and the corresponding surrogate data sets have significantly different ( $p < 0.001$ )  $D_2$  values for the entire range of embedding dimensions except for the mixed sine wave of five wave forms at embedding dimension 4 ( $p=0.1716$ ).

### C. White Gaussian noise and colored Gaussian noises

The white Gaussian noise as expected does not have saturable  $D_2$  values [Fig. 5(e)]. The surrogate sets cannot be differentiated from the original values and the  $D_2$  values of the surrogate sets are not statistically different from the original ( $p > 0.17$ ) for the entire range of embedding dimension. The colored Gaussian noises, those generated by low-pass filtering and containing low-frequency components, show saturation in their  $D_2$  values between 4 and 16 and 6 and 16 embedding dimensions for the 3 Hz and 300 Hz cutoff signals, respectively, [Figs. 5(f) and 5(g)]. The surrogate-data tests of these signals show statistically different behavior. The colored noises filtered between 3 Hz and 300 Hz have significantly different  $D_2$  values than the corresponding surrogates ( $p < 0.001$  for 3 Hz and 300 Hz low-pass cutoff). However, the colored noise signals containing high-frequency components show no saturation in their  $D_2$  curves and the  $D_2$  values of the original data sets are not significantly different from their surrogate counterparts ( $p > 0.083$ ). At the frequency cutoff of 900 Hz the signals show gross similarity with white Gaussian noise [Fig. 5(h)].

### D. EEG signals

We have analyzed a large number of segments of EEG signals from different locations of the scalp in behavioral states. In this paper, we present the surrogate-data tests of known EEG wave forms or activities. It is found that the  $\theta$  and  $\delta$  range of EEG activities pass through the surrogate testing. These have saturable  $D_2$  values and the surrogate sets are significantly different in their  $D_2$

values from their original sets ( $p < 0.001$  for  $\delta$  and  $\theta$  activities but  $p = 0.0018$  for embedding dimension 8 of  $\theta$  activity) for the entire range of embedding dimension. While there is an appreciable saturation in the  $D_2$  curves of the  $\alpha$  and  $\beta$  range of activities, the majority of these activities prove positive in surrogate testing and have a saturable or finite correlation dimension. The surrogate sets of  $\alpha$  activities have  $D_2$  values that are significantly higher than the original data sets ( $p < 0.001$  but  $p = 0.0412$  at embedding dimension 4). For the  $\beta$  activities, the surrogate sets have significantly different  $D_2$  values than the original data ( $p < 0.01$ ) for all embedding dimensions except 6 ( $p=0.0708$ ). The average correlation dimensions of  $\alpha$  and  $\beta$  activities are also higher than the  $\theta$  and  $\delta$  activities. For the indeterminate EEG activities, the surrogate sets have significantly higher  $D_2$  values than the original set ( $p < 0.05$ ) for all embedding dimensions except 6 ( $p=0.4238$ ).

We point out that when a single realization is taken the  $D_2$  value of the original data set and that of surrogate-data sets may not show significant differences in some segments of the EEG in the  $\alpha$  and  $\beta$  range of activities. For all of the  $\delta$  and  $\theta$  range of EEG activities, the  $D_2$  values of the surrogate-data sets are significantly different from that of the original signal. A test of significance may not be appropriate while comparing a single set of values of original data with many sets of values of its surrogates. Therefore these results are not included in this paper.

## V. DISCUSSION

The understanding that deterministic dynamical systems can display aperiodic behavior has strong bearing on EEG research: random-looking EEG activities may be the outcome of a chaotic process. This new approach of nonlinear dynamics to EEG's envisages deterministic rules underlying EEG generation in contrast to the traditional approach where EEG activity is considered to be due to a linear stochastic process or a filtered noise. While a number of technical problems need to be addressed for application of nonlinear dynamical measures to EEG's, criticism has cropped up about the utility of nonlinear dynamical measures of EEG's. It has stemmed from the need for a test procedure that can distinguish colored noises from chaotic processes. Surrogate-data testing has been used to detect nonlinearity and chaos in EEG [25–27]. We have evaluated the surrogate-testing procedure for chaotic time series, mixed sine waves, white Gaussian noises, colored Gaussian noises, and EEG's. Our results clearly indicate that the surrogate testing alone may not resolve such ambiguities. The test fails for colored noises of low-frequency content and mixed sine waves. These signals also have low correlation dimensions.

The Lorenz and Hénon systems are classic examples of known chaotic systems of low dimensions. The surrogate-data sets have statistically different  $D_2$  values from the original data across different embedding dimensions ranging from 4 to 16. Therefore it may be inferred that the original series are not due to linear stochastic pro-

cesses. There is no ambiguity in differentiating the low-dimensional chaotic time series and its linear stochastic counterparts resulting from surrogating the original data [Fig. 5(a)].

The mixed sine waves (a mixture of 20 sinusoidal wave forms) do not have saturation in the  $D_2$  values and the  $D_2$  increases with increase in embedding dimensions. Its behavior is like white Gaussian noise. However, unlike white Gaussian noise, the surrogate-data sets of mixed sine waves have statistically different  $D_2$  values from the original data sets. This shows that the linear stochastic counterparts of the time series may have statistically different  $D_2$  values in the absence of a limiting correlation dimension [Fig. 5(d)]. In the case of white Gaussian noise, the  $D_2$  values of the linear stochastic parts are indistinguishable from the original data sets and the surrogate test positively identifies it to be linear stochastic in the absence of a limiting correlation dimension [Fig. 5(e)]. In the case of mixed sine waves, the surrogate testing is ambiguous. The results do not differentiate it from chaotic systems and thus in the absence of other measures the surrogate testing may interpret it as chaotic. Therefore a limiting correlation dimension or saturation of the  $D_2$  value with increasing embedding may be considered as a prerequisite for identification of chaotic systems. This conjecture has been implied in the theory of chaos [36]. The saturation of  $D_2$  curves or a limiting correlation dimension have an intrinsic relation to surrogate testing in that a stochastic system does not define an attractor and the finite  $D_2$  value of any system

is a measure of its minimum number of degrees of freedom. Further, the saturation of  $D_2$  values is seen if the mixed sine waves contain fewer sine waves [Figs. 5(b) and 5(c)]. This makes the surrogate testing totally invalid as a means to detect low dimensional chaos.

For the colored noises, we have shown that at a low-frequency range up to 300 Hz of the filter setting the resulting colored signals pass surrogate testing [Figs. 5(f) and 5(g)]. These signals have limiting correlation dimensions. These forms of colored noises are mistaken as low-dimensional chaos by the test. The surrogate testing only differentiates colored noises of high-frequency content [Fig. 5(h)]. This makes the surrogate testing indeed irrelevant. Surrogate-data testing, therefore, cannot be construed as a test for detecting low-dimensional chaos.

In our study of EEG data we have extracted eight independent realizations of different EEG activity patterns. The  $D_2$  curves show saturation and limiting correlation dimensions (Fig. 6). While the  $\beta$  and indeterminate activities have saturations at high embedding, the  $\delta$ ,  $\alpha$ , and  $\theta$  activities show saturation at 6–8 embedding dimensions. The surrogate sets have  $D_2$  values that are significantly different for all embedding dimensions. These results strongly contradict the results of previous claims on surrogate testing that EEG activity is nonchaotic [26,27,29]. Almost all EEG segments have limiting correlation dimensions.

For EEG time series, physiological imperatives suggest that dynamical changes in the EEG pattern occur during sleep and other states of behavior. The EEG patterns

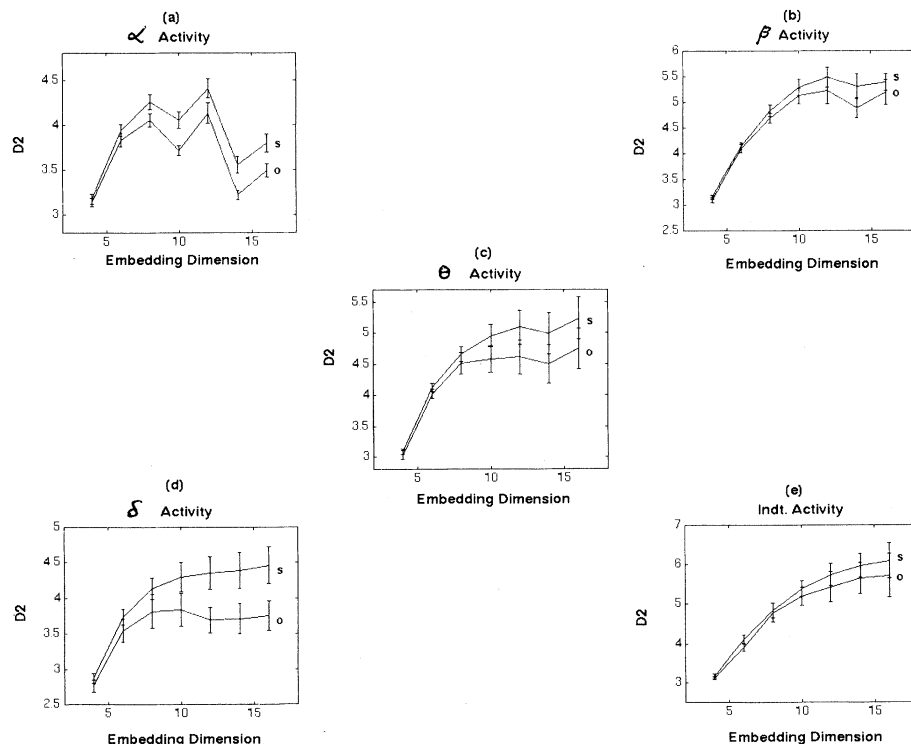


FIG. 6. The estimated  $D_2$  for original data sets (o) and the corresponding surrogate data sets (s) for the experimental EEG data of (a)  $\alpha$  activity, (b)  $\beta$  activity, (c)  $\theta$  activity, (d)  $\delta$  activity, and (e) indeterminate activity.

change from the random-looking awake state to periodic slow wave patterns in deep sleep. Therefore it is pertinent to address the brain mechanism that may produce such transitions. It is unlikely that linear stochastic brain processes produce such transitions. Our results suggest that the basic underlying brain dynamics may be chaotic. The different transitional states may be brought about by a varying degree of relaxation of the control mechanisms. This may account for transitions to different chaotic regimes of varying dimensional complexities [37]. The brain activity in high-dimensional states may be approximated by linear stochastic processes.

The nature of randomlike signals such as EEG's that arise from a dissipative dynamical system may be chaotic in nature and may display varying dimensions depending on the control parameters that govern the degrees of freedom of the system. It is known that oscillations in single neuron and neuronal ensembles underlie the generation of various pattern features in EEG's. Since mathematicians have long known that the periodic forcing of nonlinear oscillators can give rise to complex phase locking patterns, bifurcations, and aperiodic dynamics [38], one anticipates that such behavior might be observable in forced neuronal oscillators. Studies on the periodic forcing of biological oscillators have, in fact, been interpreted in the context of chaotic dynamics [39]. It has been proposed that complex EEG patterns which occur normally arise from interactions between a large number of neural relaxation oscillators [40]. All these observations raise the possibility that some of the observed variability in neural electrical activity may be a reflection of intrinsically chaotic dynamics.

From the results of analysis of a large number of segments of EEG data, we put forth the following practical considerations for EEG analysis.

(1) It is premature to conclude that "EEG activity is nonchaotic and at best nonlinear or it is due to a linear stochastic process" or "colored noise." Notwithstanding the mechanism of EEG activity being a linearly correlated noise or stochastic process, it has a finite correlation dimension and positive Lyapunov exponents. It has been repeatedly reproduced in the literature by a large number of research groups [13,40]. A parallelism between the attractor dimension and the  $\lambda_1$  curve in our earlier studies may be seen as indirect evidence for the Kaplan-York conjecture to be true for EEG data [41]. It is not clear how "surrogate testing" would be valid for systems

exhibiting dimensions  $> 3$ . Our study suggests that the attractor of chaotic systems (dimensions  $> 8$ ) is likely to be near stochastic regimes. The phase space may have a near random distribution. Any phase scrambling will not lead to a positive surrogate test. We have found similar trends in testing single blocks of EEG data in the  $\alpha$  and  $\beta$  range of activities.

(2) Unlike a dominant positive Lyapunov exponent, surrogate testing is not a definite criterion for testing chaos. It may only distinguish very low-dimensional (dimension  $< 5$ ) chaotic signals from very high-frequency colored noises. Therefore, surrogate-data testing should not be considered as a valid test for chaos. A limiting correlation dimension and at least one positive Lyapunov exponent may be sufficient to characterize chaos.

## VI. CONCLUSION

From the studies on surrogate testing it is difficult to prove the claim that EEG signals are colored noises having finite correlation dimension. It is difficult to sustain the argument that EEG activity needs to be unequivocally proved to be chaotic by "surrogate testing." Surrogate-data testing may not distinguish chaotic time series and colored noises of low-frequency content. Given a finite correlation dimension, it is difficult to resolve whether it is of a strange attractor or a chaotic process. This may be a valid question for those who adhere to stochastic descriptions of dissipative dynamical systems. There is no short answer to this question by surrogate testing as of now. An indirect and partial answer is in Mandelbrot's remark that if any natural process were a fractional Brownian motion (fBm), it would have grown enough to destroy nature. From the clinical and physiological evidences we assume that the EEG is not noise or filtered noise. The transitions seen in the normal waking state EEG's, normal sleep EEG's and other behavioral states call for alternate explanations and thus the chaotic conjecture of EEG generation is appealing.

## ACKNOWLEDGMENTS

This work has been supported by a grant from the Department of Biotechnology (BT/R&D/09/48/92), Government of India.

- 
- [1] P.E. Rapp, I.D. Zimmerman, A.M. Albano, G.C. deGuzman, N.N. Greenbaum, and T.R. Bashore, in *Nonlinear Oscillations in Biology and Chemistry*, edited by H.G. Othmer (Springer, Berlin, 1986), p. 175.
  - [2] A.M. Albano, A.I. Mees, G.C. deGuzman, and P.E. Rapp, in *Chaos in Biological Systems*, edited by H. Degn, A.V. Holden, and L.F. Olsen (Plenum, New York, 1987).
  - [3] T.M. McKenna, T.A. McMullen, and M.F. Shlesinger, *Neuroscience* **60**, 587 (1994).
  - [4] E. Basar, *Chaos in Brain Function* (Springer-Verlag, Berlin, 1990).
  - [5] I. Dvorak and A.V. Holden, *Mathematical Approaches to Brain Functioning Diagnostics* (Manchester University Press, Manchester, 1991).
  - [6] B.H. Jansen, *Int. J. Biomed. Comput.* **27**, 95 (1991).
  - [7] B.H. Jansen, in *Measuring Chaos in the Human Brain*, edited by D.W. Duke and W.S. Pritchard (World Scientific, Singapore, 1991).
  - [8] A. Babloyantz, J.M. Salazar, and C. Nicolis, *Phys. Lett.* **111A**, 152 (1985).



- [9] A. Babloyantz and A. Destexhe, Proc. Natl. Acad. Sci. U.S.A. **83**, 3513 (1986).
- [10] I. Dvorak, J. Siska, J. Wackermann, L. Hrudova, and C. Dostalek, Act. Nerv. Super. **28**, 228 (1986).
- [11] P.E. Rapp, T.R. Bashore, J.M. Martinerie, A.M. Albano, I.D. Zimmerman, and A.I. Mees, Brain Topography **2**, 99 (1989).
- [12] T. Elbert, W.J. Ray, Z.J. Kowalik, J.E. Skinner, K.E. Graf, and N. Birbaumer, Phys. Rev. **74**, 1 (1994).
- [13] *Nonlinear Dynamical Analysis of the EEG*, edited by B.H. Jansen and M.E. Brandt (World Scientific, Singapore, 1993).
- [14] S.P. Layne, G. Mayer-Kress, and J. Holzfuss, in *Dimensions and Entropies in Chaotic Systems*, edited by G. Mayer-Kress (Springer, New York, 1986), p. 246.
- [15] G. Mayer-Kress and S.P. Layne, in *Perspectives in Biological Dynamics and Theoretical Medicine*, edited by S.H. Koslow, A.J. Madel, and M.F. Shlesinger (New York Academy of Sciences, New York, 1987), p. 62.
- [16] X. Nan and X. Jinghua, Bull. Math. Biol. **50**, 559 (1988).
- [17] R.C. Watt and S.R. Hameroff, in *Perspectives in Biological Dynamics and Theoretical Medicine*, edited by S.H. Koslow (New York Academy of Sciences, New York, 1987), p. 286.
- [18] N. Birbaumer, W. Lutzenberger, and H. Flor, Psychophysiology **29**, S19 (1992).
- [19] R.A.M. Gregson, E.A. Campbell, and G.R. Gates, Biol. Psychol. **35**, 165 (1992).
- [20] J. Roschke, K. Mann, and J. Fell, Int. J. Neurosci. **75**, 271 (1994).
- [21] J.C. Parikh and R. Pratap, Pramana J. Phys. **3**, L347 (1991).
- [22] N. Pradhan and D. Narayana Dutt, Comput. Biol. Med. **23**, 425 (1993).
- [23] D. Gallez and A. Babloyantz, Biol. Cybernetics **64**, 381 (1991).
- [24] A.M. Albano and P.E. Rapp, in *Nonlinear Dynamical Analysis of the EEG* [13], p. 117.
- [25] J. Theiler, S. Eubank, A. Longtin, B. Galdrikian, and J.D. Farmer, Physica D **58**, 77 (1992).
- [26] L. Glass, D.T. Kaplan, and J.E. Lewis, in *Nonlinear Dynamical Analysis of the EEG* [13], p. 233.
- [27] W.S. Pritchard, D.W. Duke, and K.K. Kriebel, Psychophysiology, **32**, 486 (1995).
- [28] A.R. Osborne and A. Provenzale, Physica D **35**, 357 (1989).
- [29] M. Palus, Santa Fe Institute Report No. 94-10-054, 1994 (unpublished).
- [30] J.P. Pijn, J. van Neervan, A. Noest, and F.H. Lopes da Silva, Electroencephalogr. Clin. Neurophysiol. **79**, 371 (1991).
- [31] P.E. Rapp, Biologist **40**, 89 (1993).
- [32] P.E. Rapp, A.M. Albano, T.I. Schmah, and L.A. Farwell, Phys. Rev. E **47**, 2289 (1993).
- [33] A. Rechtschaffen and A. Kales, *A Manual of Standardized Terminology, Technique and Scoring for Sleep Stages of Human Subjects*, Public Health Services (U.S. GPO, Washington, DC, 1968).
- [34] F. Takens, *On the Numerical Determination of the Dimension of an Attractor*, edited by B. L. J. Braaksma, H. W. Broer, and F. Takens, Lecture Notes in Mathematics Vol. 1125 (Springer-Verlag, Berlin, 1985), p. 99.
- [35] S. Ellner, Phys. Lett. A **133**, 128 (1988).
- [36] H.G. Schuster, *Deterministic Chaos. An Introduction*, 2nd revised ed. (VCH, New York, 1988).
- [37] N. Pradhan, P.K. Sadasivan, S. Chatterji, and D. Narayan Dutt, Comput. Biol. Med. **25**, 455 (1995).
- [38] C. Hayashi, *Nonlinear Oscillations in Physical Systems* (McGraw-Hill, New York, 1964).
- [39] N. Hayashi, M. Nakao, and N. Hirakawa, Phys. Lett. **88A**, 265 (1982).
- [40] E. Basar, *Chaos in Brain Function* (Springer-Verlag, Berlin, 1990).
- [41] N. Pradhan and P.K. Sadasivan (unpublished).